E. N. P.

𝕬𝖗𝖌𝖔𝖓𝖓𝖊 𝕹𝖆𝖙𝖎𝖔𝖓𝖆𝖑 𝕷𝖆𝖇𝖔𝖗𝖆𝖙𝖔𝖗𝖞

CRITICAL EXPERIMENT WITH BORAX-V

Internal Superheater

by

K. E. Plumlee, Q. L. Baird, G. S. Stanford, and P. I. Amundson

ARGONNE NATIONAL LABORATORY
9700 South Cass Avenue
Argonne, Illinois 60440

CRITICAL EXPERIMENT WITH BORAX-V

Internal Superheater

by

K. E. Plumlee, Q. L. Baird, and G. S. Stanford
Reactor Physics Division

and

P. I. Amundson
Idaho Division

November 1963

TABLE OF CONTENTS

TABLE OF CONTENTS

LIST OF FIGURES

LIST OF TABLES

4

CRITICAL EXPERIMENT WITH BORAX-V

Internal Superheater

by

K. E. Plumlee, Q. L. Baird, G. S. Stanford,
and P. I. Amundson

ABSTRACT

A critical experiment was performed with 12 BORAX-V superheater subassemblies in a central voidable region plus 1228 to 1525 UO_2 fuel pins (3 w/o enriched) in a peripheral region. Removing water (28% of superheater volume) at room temperature decreased reactivity by 2.2%. The midplane (two-dimensional) peak-to-average power distribution in the voided superheater was approximately 1.24, mostly attributable to flux depressions within insulated fuel boxes. Cadmium ratios are also reported. The experiment was initiated to supplement computational information which might have affected plans for loading the superheater zone into the BORAX-V reactor. No changes were indicated by the experiment.

I. INTRODUCTION

The critical experiment with BORAX-V Internal Superheater[1] was carried out to provide preliminary information needed before loading the superheater into the BORAX-V reactor. Among considerations affecting the decision to do a critical experiment separately from the power reactor were the following:

1. The information was needed before loading the superheater subassemblies into the power reactor, since it might have affected plans for the loading.

2. Components could be installed in a much more accessible condition in the critical experiment than in the BORAX-V facility. For example, the twelve superheater subassemblies were used in the critical experiment before transition pieces were welded to the ends. It appeared much more difficult to take extensive foil measurements in the completed subassemblies. Eventually, there were supplementary measurements in the BORAX-V reactor as well.

3. The critical experiment was run concurrently during operation of the power reactor with a boiling (nonsuperheating) core, thus shortening the schedule.

The information most desired was power distribution. Secondary interests were spectrum information and void worths. Control rod calibrations were also made.

II. SUMMARY

Data from the BORAX-V Superheater Critical Experiment indicated a generally flat, central power distribution at the midplane, but having superimposed perturbations of impressive size. Radial epicadmium fission activation measurements in the 28% voided superheater dropped only 7% below the central level, and ripples at the interface with the boiling zone reached as high as the central activation. This radial shape contributed a factor of ~1.02 to the peak-to-average ratio in the superheater region.

Subcadmium flux perturbations within the insulated fuel elements resulted in a fission distribution having an edge-to-average ratio of 1.22 in the direction parallel with the fuel plates and an outside fuel plate-to-average ratio of ~1.07 in the direction normal to the fuel plates. This indicated that a contribution of 1.30 to the midplane (two-dimensional) maximum-to-average fission probability in U^{235} (i.e., fission rate per unit mass, since composition varied) was attributable to the local flux perturbation associated with each insulated fuel element. Since the outer fuel plates of each four-plate element have reduced fuel concentration, only the factor 1.22 applies in terms of power distribution.

The flux ripple located in the moderator between boxes peaked to ~1.07 times the flux at the surface of the insulating boxes, yielding an average factor of about 1.04. A factor of 1.05 was measured between the outer surface of boxes and the nearest enclosed fuel plates.

The assumption of spatial separability of flux components appeared to be applicable to the plots of local perturbations inside insulating boxes. The flux shape on the surface of an insulating box appeared the same as the shapes found between the fuel plates inside the box (i.e., in parallel planes).

Voiding by displacement of moderator in the central superheater resulted in 2.2% loss of reactivity ρ for 28% void. The coefficient varied with location and with the status of the core. The installation of a voided central safety element sheath between quadrants of the voided superheater

resulted in a negligible loss of reactivity. If of equal importance with void in the remainder of the superheater region, a loss of at least 0.2% ρ would have been found. However, the reactivity losses attributed to voiding of individual quadrants all fell between 0.4% and 0.6% ρ. A somewhat similar measurement in the BORAX-V facility was reported to have given a slightly smaller loss. A loss of 1.0 ± 0.1% ρ was reported for voiding approximately 19% of the superheater, by volume. However, only the coolant channels (and not the insulating channels) were voided, which were at lower than average flux. This figure varied by as much as 0.2%, depending on the position of the central cruciform control element.

Interest in spectral information led to measurements of cadmium ratios for the activations of Au, Dy, Cu, In, Lu^{175}, Lu^{176}, Mn, and U^{235} (fissions) at six positions in the superheater and seven in the peripheral zone, in the midplane. The cadmium ratio for infinitely thin gold was ~1.2, indicating that the spectrum was hard enough that a Maxwellian energy distribution does not apply and, consequently, neither does the Westcott cross-section convention.

III. MIDPLANE FLUX DISTRIBUTION MEASUREMENTS

A. Epicadmium Activity Measurements

Epicadmium activity measurements were plotted in Fig. 5 for U^{235} fission, Cu, Mn, In, and Au as a function of radius alone. The data were normalized to central bare foil activities set to unity. The irradiations were during voided operation. Distinctive points were found in the following locations: (1) The interface between superheater and peripheral regions was the location of a ripple in the activation plot for each detector. Suprising dissimilarities were noted between various detectors. (2) The corner of the peripheral zone which projected into the superheater was the site of the highest fission rate of the peripheral zone. This is also evident in Fig. 6. (3) The flat sides of the peripheral zone fuel (control blade locations) produced a depression in each radial traverse, which is indicated by the lower dashed line (for foil placement, see Fig. 14 below). The core description is given in Section VIII and in Figs. 1-4.

The epicadmium fission activity measurement was within 7% of the central maximum at all points, and the estimated peak-to-average ratio from those data was ~1.02 when weighted by area represented in the radial plot, for the voided superheater.
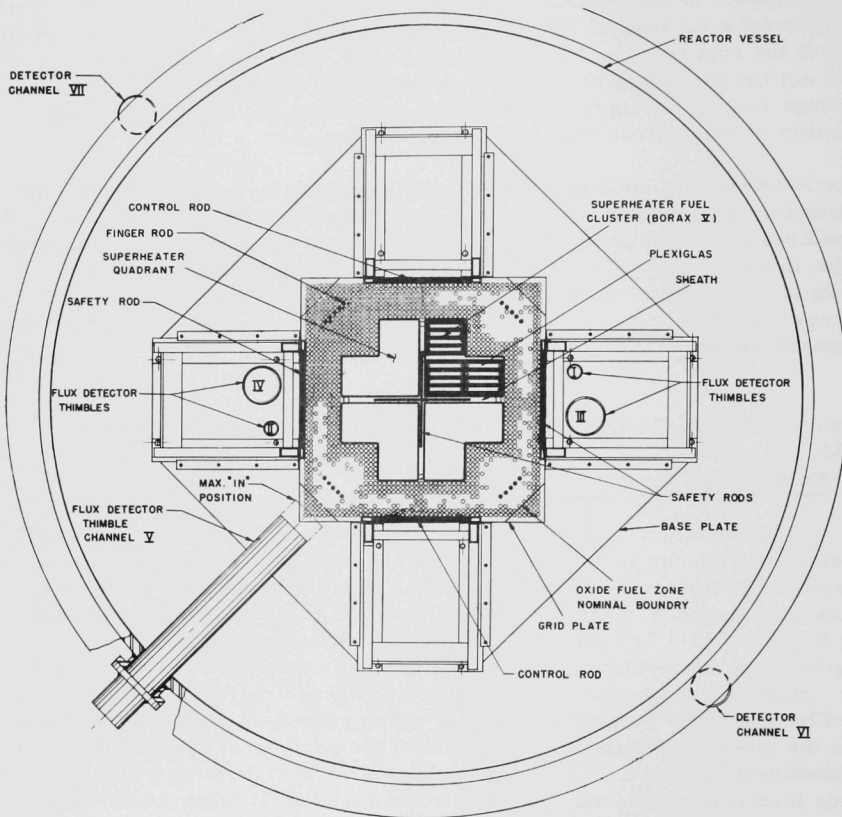
Fig. 1. Central Superheater Core - plan view
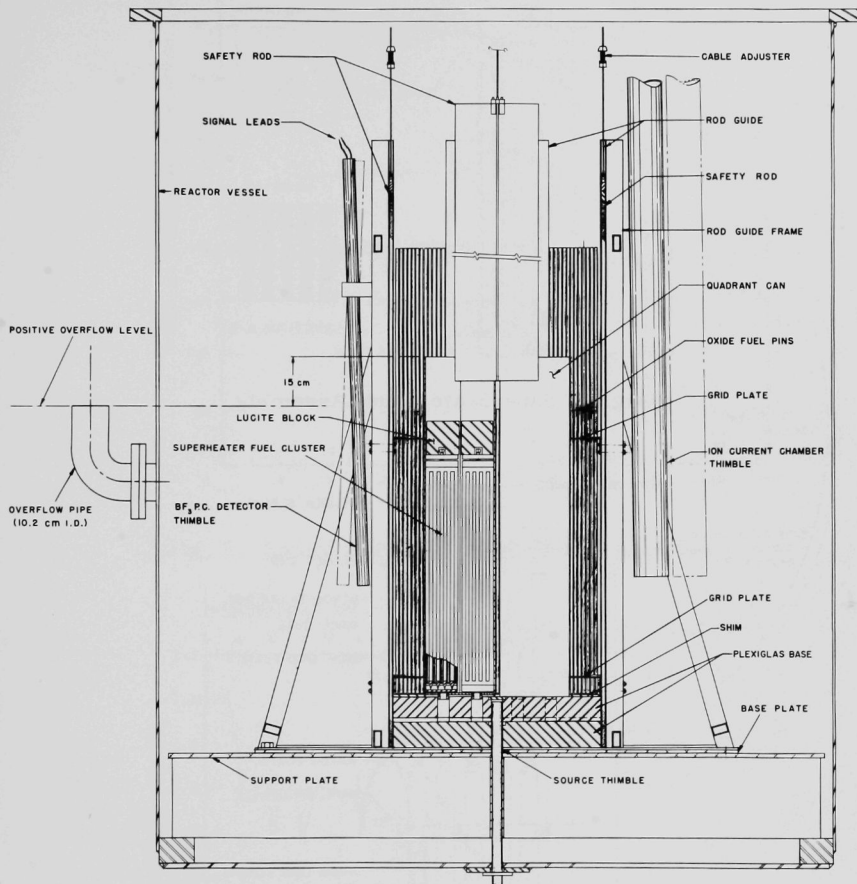
Fig. 2. Central Superheater Core - sectional view
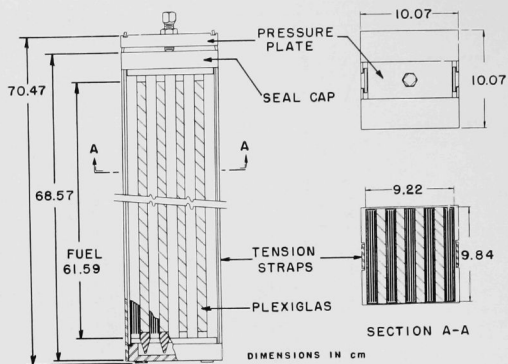
Fig. 3. Superheater Fuel Assembly
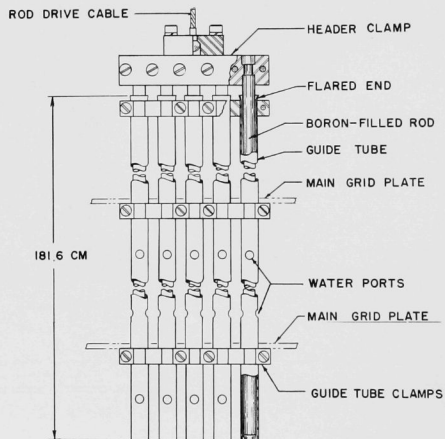
Fig. 4. Finger-type Safety Rod
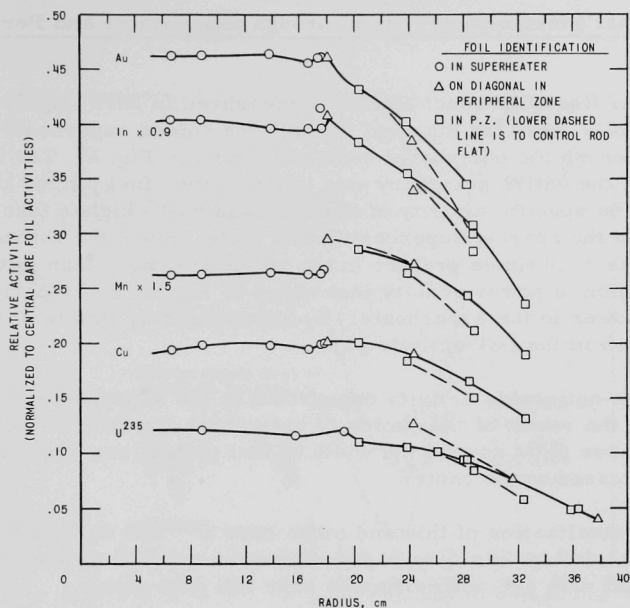
Fig. 5. Radial Epicadmium Activity Traverses
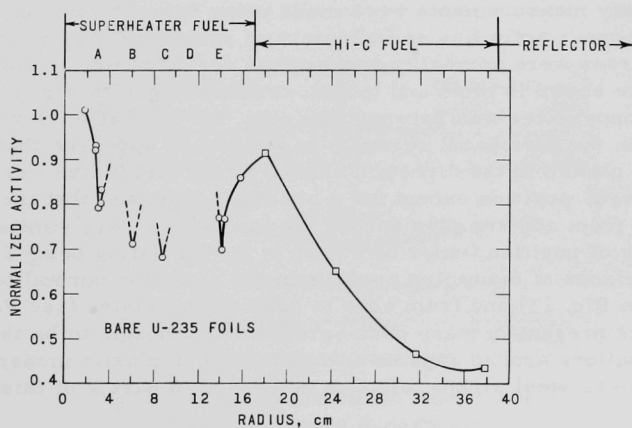
Fig. 6. Diagonal U^{235} Foil Traverse through
Superheater and Peripheral Zones

B. Diagonal Fission Distribution through Superheater and Peripheral Zones

The fission product activities measured in bare, highly enriched uranium foils along the diagonal through the voided superheater and extending through the peripheral zone are shown in Fig. 6. The highest activity in the entire periphery was in the corner fuel pin, at an 18-cm radius. The specific activity of that foil was ~10% higher than of the foil next to the nearest superheater fuel plate. Since the average U^{235} density was ~1.9 times greater in the peripheral zone than in the superheater region, a power density plot would be higher in the peripheral zone (or lower in the superheater) by approximately this factor of 1.9 than is seen in the foil-activity plot.

The noticeable activity depression in the superheater region is primarily the result of the choice of a diagonal direction. The edge-to-edge traverse plots across the width of fuel plates (see Figs. 11-13 below) were depressed at the center.

Normalization of this and other bare U^{235} foil data plots was common so that data points may be transferred from plot to plot. Cadmium-covered foil data are normalized to bare foil data plots.

C. Distributed Measurements in Superheater and Peripheral Zones

Many measurements were made using bare U^{235} fission activities and bare copper activities as indicators of power and flux distributions. The traverses were normalized as well as appeared practicable. The results are shown in plots and tables, commencing with Fig. 7. (Note that the copper wire was between fuel pins, but the flat foils were inside fuel pins in the peripheral region.) In general, it appeared that the traverses plotted in the direction normal to the fuel plates were independent of lateral position except for a scaling factor, and that the lateral traverses from edge to edge across the fuel plates were similar in shape regardless of position (inner or outer) in the insulating box. This is shown by comparisons of many flux profiles in the direction normal to the fuel plates (see Fig. 13) and from edge to edge of fuel plates (see Fig. 11). Distortions present in many of the profiles are thought to be the result of perturbations around gaps or irregularities in plastic moderator material, stainless steel straps, etc., as discussed in part V of this report.

The available data appeared consistent with the assumption of spatial separability of flux components. Small differences in shape may not have been evident because of data scatter.
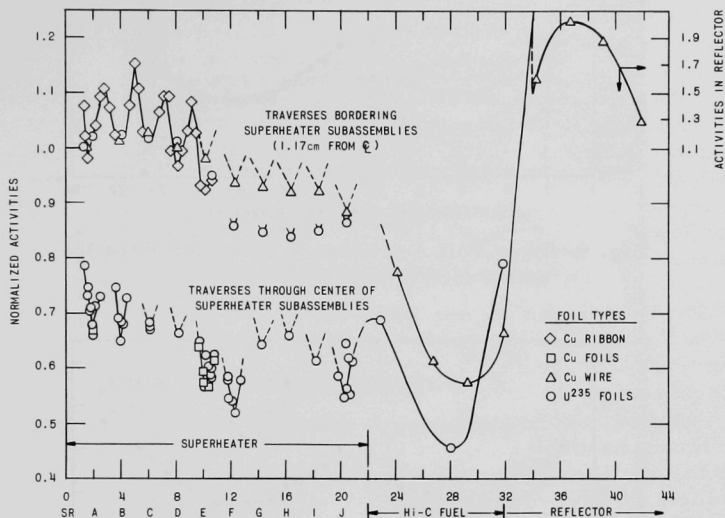
Fig. 7. Traverses Normal to Superheater Fuel Plates
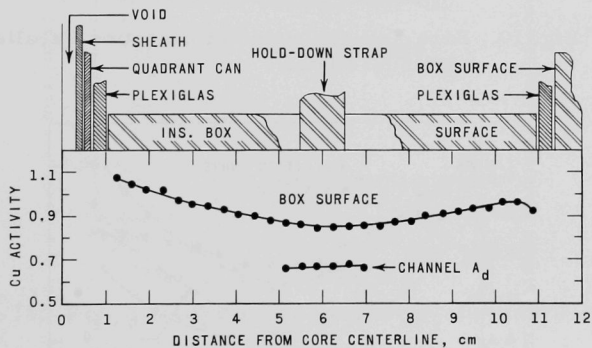
Fig. 8. Exterior Traverse Parallel to
Fuel Plates of Superheater

14
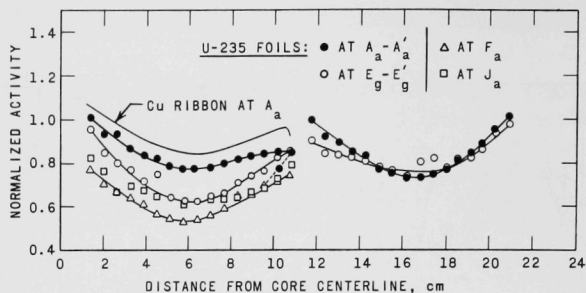
Fig. 9. Bare Foil Activities in Direction Parallel with Fuel Plates
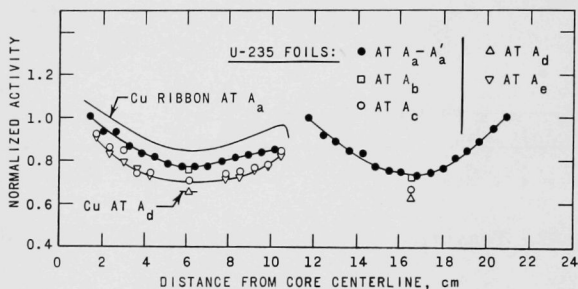
Fig. 10. Bare Foil Activities in Direction Parallel with Fuel Plates
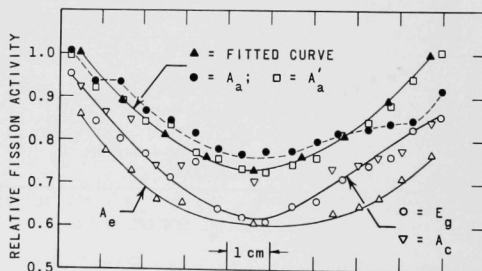
Fig. 11. U^{235} Foil Activity Depression Through Insulating Box in Direction Parallel with Fuel Plates
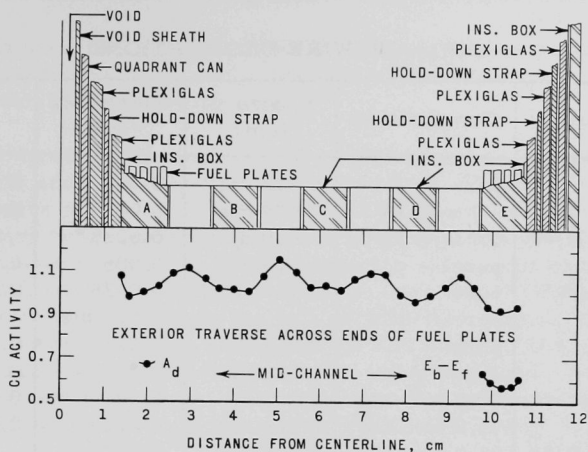
Fig. 12. Exterior Traverse Across Ends of Fuel Plates
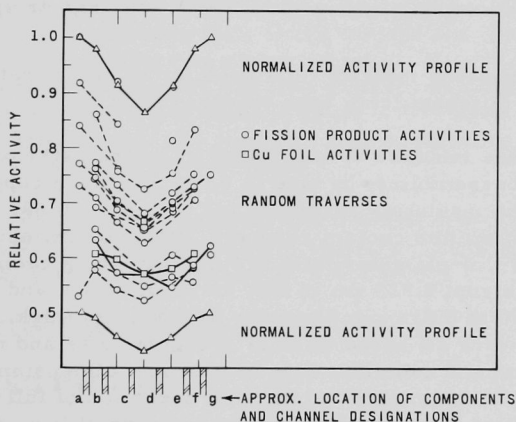
Fig. 13. Foil Activity Depression through Insulating Box

D. Description of Materials for Flux Detection

The foil materials listed in Table I were used during measurements of flux distributions in the central superheater critical experiments.

Table I

FOIL AND WIRE DESCRIPTIONS

Material	Composition	Size (cm)	Thickness (cm)	Weight (g)
Au	pure	0.818 dia	0.0025	0.028
Dy-Al	3.7 w/o Dy	0.584 dia	0.0023	0.017 ± .001
Dy-Al (Cd R)**	3.7 w/o Dy	0.919 dia	0.0023	-
Cu	pure	0.818 dia	0.005	0.023
(Cu Ribbon)*	pure	3.75 x 0.38	0.0025	0.050 ± .008
(Cu Wire)	pure	-	0.127 dia	-
In	pure	0.818 dia	0.0025	0.011
Lu-Al	2.5 w/o Lu	0.818 dia	0.025	0.036
Mn-Cu	90.0 w/o Mn	0.818 dia	0.005	0.020 - .023
Enr U	93.0 w/o U^{235}	0.584 dia	0.0025	0.012 ± .001
Enr U (Cd R)**	93.0 w/o U^{235}	0.818 dia	0.0025	

*Cu ribbon was clipped to 0.38-cm strips after activation. The narrow pieces were counted separately for higher spatial resolution.

**(Cd R) notations indicate foils used for cadmium ratio measurements if different from bare traverse foils.

Foils were mounted by tape (Mystic) on the exterior surfaces of the superheater subassemblies; by tape to 0.005-cm-thick copper strips for insertion into the insulating channels; and by tape to 0.081-cm-thick Teflon strips for insertion into coolant channels. All epicadmium measurements were with 0.818-cm-diameter foils in 0.051-cm-thick cadmium covers which included a cup, 0.928 cm in OD, 0.818 cm in ID, and ~0.060 cm deep inside, plus a lid of 0.818-cm diameter by 0.051 cm thick. Cadmium ratio measurements were all based on foils of a given size and material irradiated in aluminum and cadmium cups of identical dimensions. Some superheater coolant channels were too tight for insertion of full-size cups, and the cups were filed to the minimal thickness overall (i.e., 0.10 cm) of the two thicknesses of cadmium plus a thin foil sandwiched between.

Foils were inserted into slotted Hi-C fuel pins and the UO_2 fuel pellets were snugly butted against the aluminum or cadmium covers housing the foils.

A few measurements in the peripheral fuel region were outside rather than inside the fuel elements. These included the copper wire of Fig. 7.

IV. FLUX PERTURBATIONS IN SUPERHEATER FUEL ELEMENTS

The largest flux irregularities in the superheater region were the local flux depressions in the fuel elements. The foil activations were averaged to obtain the following shapes:

In the direction normal to the fuel plates, it was estimated (from data similar to and including those plotted in Figs. 12 and 13) that a normalized value of 1.07 applied to the peak in the moderator slab between insulating boxes, unity at the outer surface of the insulating box; 0.98 in the insulating channel; 0.91 between the outer, half concentration enriched (HCE) and inner, full concentration enriched (FCE) fuel plates; and 0.86 in the channel between the pair of FCE fuel plates. Figure 13 shows a number of traverses normal to the fuel plates. The top and bottom plots are the estimated fit scaled to unity (top) and 0.5 (bottom) at the exterior surfaces of the insulating box. The structure and the components of an insulating box have been indicated in Fig. 3.

Assignment of values corresponding either to a peak-to-average ratio or to a disadvantage factor is complicated by the difference in fuel composition in HCE (outer) and FCE (inner) fuel plates. The measurements were made by irradiating foils in the coolant and insulating channels, rather than by sampling fuel plates directly. Nevertheless, the plotted points were nearly linear, and interpolation was used in estimating fuel plate activation. On an interpolated basis, a U^{235} atom in an outer (HCE) fuel plate should have 1.07 times as high probability of fission as it would have in an inner (FCE) fuel plate.

The fit in the direction parallel with the fuel plates (i.e., edge-to-edge) was made with an equation $F(x)$, where x is the distance from one edge of a fuel plate having a width $W = 9.2$ cm:

$$F(x) = G\{\exp(-xc) + [\exp(xc)][\exp(-wc)]\} \quad .$$

The solutions for G and C are

$$G = \frac{F(o) \mp F\left(\frac{W}{2}\right)}{\left[1 \mp \exp\left(-\frac{WC}{2}\right)\right]^2}$$

Note that both signs are negative or both are positive, yielding only one value of G.

$$C = \frac{2}{W} \ln_e \left[\frac{Z+1}{1-Z}\right]$$

$$Z = \left[\frac{F(o) - F\left(\frac{W}{2}\right)}{F(o) + F\left(\frac{W}{2}\right)}\right]^{1/2} \quad .$$

The average value $\overline{F}$ of $F(x)$ is

$$\overline{F} = \frac{2}{WC} [2G - F(o)] \quad .$$

Typical traverses across the fuel plates are shown along with the fitted curve in Fig. 11. The fitted curve gave a value $\overline{F} = 0.818$ of the edge activation, which is equivalent to an edge-to-average ratio of 1.22.

The equation above was found to fit the data reasonably well. The equation is the sum of two symmetrically positioned attenuation curves. The use of such an equation was suggested by the exponential form of solutions for flux diffusion from a plane source, as found in standard texts. The surrounding moderator was considered to serve as source planes enclosing the moderator-free insulating boxes. The solutions for G (an amplitude) and C were chosen to minimize the effects of random measuring errors.

Simpler formulae failed to match the curvature indicated by data plots. A more complicated formula appeared to yield equivalent results. Specifically, the inclusion of a nonattenuated component produced a near-zero coefficient for this component.

V. CADMIUM RATIO MEASUREMENTS

Cadmium ratios were measured at thirteen locations in one quadrant of the core, indicated in Fig. 14. Each measurement in the superheater zone was made inside a voided fuel cluster with the foil capsules mounted on Teflon strips. In the peripheral zone, the foils were in fuel pins, sandwiched between fuel pellets. All cadmium-covered foils were enclosed in capsules of 0.05-cm (0.02-in.) cadmium, and the "bare" foils were in similar capsules made of aluminum. For each run, two foils, one bare and one cadmium-covered, were exposed at each location; these foils were in flux-symmetrical positions, separated by a vertical distance of 5.1 cm. Cadmium ratios were determined for activation of In^{115}, Au^{197}, Mn^{55}, Cu^{63}, Lu^{175}, Lu^{176}, and Dy^{164}. For description of the foils, see Table I.

POS.	X	Y		POS.	X	Y
1	16.51	12.70		8	17.11	2.62
2	16.51	17.78		9	17.11	6.95
3	16.51	22.86		10	6.95	2.62
4	16.51	27.94		11	6.95	6.95
5	6.35	22.86		12	6.95	13.01
6	6.35	27.94		13	6.95	17.11
7	12.70	12.70		DIMENSIONS IN cm		

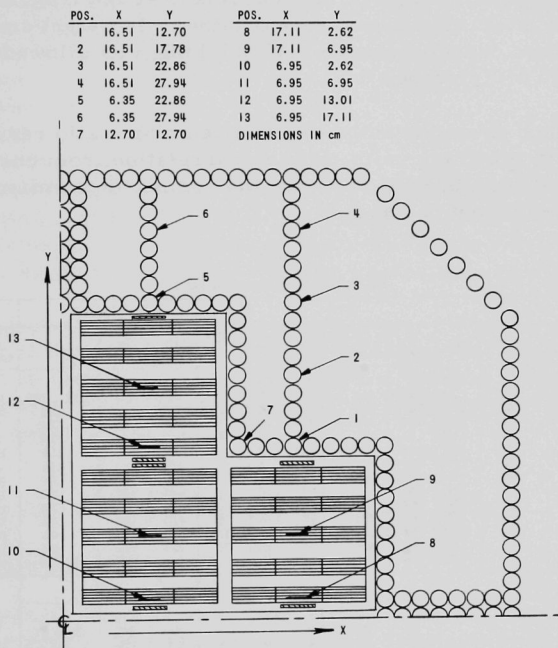Fig. 14. Foil Placement for Cadmium
Ratio Measurements

All foils were gamma counted and some were simultaneously beta counted. The data were processed by the IBM-704 code RE-202,[2] which computes the relative saturated activity by correcting for counting-system dead time, background, and decay during and after irradiation. The lutetium foils were counted shortly after irradiation to determine the Lu^{175}

activation (3.7-hr half-life) and again in several days for the Lu^{176} activation (6.8-day half-life); the first count was corrected for the contribution due to Lu^{176} as deduced from the second count.

The counting precision was typically better than 1%, exceptions being cadmium-covered Lu^{176} (~3%) and the gamma count of the dysprosium, which was so low as to be unusable. Several counts of each foil were made by an automatic foil-changing system[2] with IBM punched-card readout.

Matched foils were not used. The results for the manganese and copper activation were weight-corrected by dividing by the weight of the foil. The lutetium and dysprosium foils were intercalibrated by activation on a rotating wheel in a fairly thermal flux near the front face of the ATSR;* both β and γ intercalibrations were obtained. In weight correcting the gold and indium data, resonance self-shielding was allowed for according to the method of Reference 6.

Table II gives the activation and cadmium ratio results. The activations are in arbitrary units, with no correlation from one material to the next. The columns labeled CdR give the computed cadmium ratios for foils of the type described in Table I.

Table II

FOIL ACTIVATIONS AND CADMIUM RATIOS

Position	Lu^{115}				Au^{197}				Position	Lu^{175}			Lu^{176}		
	Al-covered	Cd-covered	CdR	CdR$_\infty$	Al-covered	Cd-covered	CdR	CdR$_\infty$		Al-covered	Cd-covered	CdR	Al-covered	Cd-covered	CdR
			±0.010	±0.005			±0.015	±0.008				1.107 ± 0.007			11.5 ± 0.8
1	1650	1034	1.596	1.226	7086	4354	1.627	1.244	1	4221	3814	1.107 ± 0.007	1377	119	11.5 ± 0.8
2	1408	929	1.516	1.192	5934	3900	1.522	1.203	2	3850	3500	1.100	1096	109	10.0
3	1244	822	1.513	1.192	5194	3460	1.501	1.194	3	3434	3173	1.082	964	101	9.5
4	985	638	1.544	1.204	-	-	-	-	4	2585	2377	1.088	798	116	6.9
5	1550	957	1.619	1.235	6669	4064	1.641	1.250	5	3993	3549	1.125	1335	122	10.9
6	1078	706	1.527	1.197	4543	3022	1.503	1.195	6	2975	2702	1.101	880	110	8.0
7	1847	1095	1.687	1.263	7818	4635	1.687	1.268	7	4514	3924	1.150	1668	140	11.9
8	1589	1068	1.488	1.181	6795	4597	1.478	1.185	8	4410	3997	1.103	1239	125	9.9
9	1575	1069	1.473	1.175	6677	4666	1.431	1.167	9	4276	4005	1.068	1203	139	9.0
10	1684	1104	1.525	1.197	6971	4676	1.491	1.190	10	4333	3973	1.091	1315	125	10.5
11	1602	1094	1.464	1.171	6924	4713	1.469	1.182	11	4365	4016	1.087	1275	125	10.2
12	1528	1071	1.427	1.156	6516	4666	1.396	1.153	12	4155	3950	1.052	1116	128	8.7
13	1605	1120	1.433	1.158	6689	4684	1.428	1.166	13	4360	4040	1.079	1230	125	9.8

Position	Mn^{55}			Cu^{63}				Dy^{164}			
	Al-covered	Cd-covered	CdR	Al-covered	Cd-covered	CdR	CdR$_\infty$	Position	Al-covered	Cd-covered	CdR
			4.26 ± 0.02			±0.05	±0.05				24.9 ± 0.4
1	7302	1715	4.26 ± 0.02	906	225	4.02	3.77	1	7369	2965	24.9 ± 0.4
2	5875	1645	3.57	724	215	3.36	3.16	2	5520	2694	20.5
3	5148	1465	3.51	635	190	3.34	3.15	3	4809	2303	20.9
4	4187	1123	3.73	517	148	3.49	3.28	4	3954	1777	22.3
5	7104	1591	4.46	856	207	4.14	3.88	5	7102	2705	26.3
6	4614	1265	3.65	571	169	3.37	3.17	6	4382	1988	22.0
7	8756	1770	4.95	1070	227	4.70	4.39	7	9263	3092	30.0
8	6100	1566	3.89	763	220	3.46	3.25	8	6039	2866	21.1
9	5802	1575	3.68	730	223	3.28	3.09	9	5499	2904	18.9
10	6522	1565	4.17	820	217	3.78	3.55	10	6493	3068	21.2
11	6162	1581	3.90	763	224	3.40	3.20	11	5973	3152	18.9
12	5448	1566	3.48	682	223	3.06	2.89	12	5053	2867	17.6
13	5918	1582	3.74	743	224	3.32	3.13	13	5698	3095	18.4

Note: For foil positions, see Fig. 14.

*Argonne Thermal Source Reactor.

For gold, indium, and copper, the "infinite-dilution" cadmium ratio CdR_∞ was determined by means of the formula

$$CdR_\infty = 1 + Q\left(\frac{CdR}{F} - 1\right) \quad ,$$

where F is a correction factor for epicadmium absorption in the 0.05-cm cadmium covers, Q is to extrapolate to zero foil thickness, and CdR, listed in Table II, is uncorrected for epicadmium absorption by the cadmium. The values used were as follows:

Foil Material	Q		F	
	Value	Ref.	Value	Ref.
In	0.435	7	1.051	4
Au	0.400	5	1.01	3
Mn	1.00	7	1.00	-
Cu	0.916	5	1.00	-

The errors shown for CdR_∞ do not include any possible systematic error in determining CdR_∞ from CdR. No correction was made for sub-cadmium transmission by the cadmium, since in all cases the correction would have been small as compared with the experimental uncertainties.[3,4]

For manganese, lutetium, and dysprosium, extrapolation to zero thickness does not involve appreciable corrections, with the possible exception of Lu^{176}, for which there is disagreement between References 7 and 8: the correction to $(CdR-1)$ would be zero from Reference 8, but a 9% reduction is called for by Reference 7.

VI. SOURCES OF ERROR IN FOIL DATA

A. Error in Activation Measurements

The standard deviation of individual activation datum points is estimated to be 2 or $2\frac{1}{2}$% in this report. The sources of error were evaluated as follows:

1. Counting statistics were generally good, and standard deviations were 0.5-1.0%, with the exception of a fraction of the data for which activations were low or counting was delayed. Low-activation levels were unavoidable in the extremities of axial traverses and in mixed (bare and cadmium-covered) traverses, where it was considered necessary to irradiate full traverses and to count the foil activities of a traverse in sequence.

The alternative would have been to irradiate or to count the activities in two or more separate operations. This would have improved counting statistics, but would have required an additional step or normalization and/ or an added intercalibration which would have overcome any improvement obtained in counting statistics.

2. Calibration drifts were significant during the counting of large numbers of foils. Although drift corrections were made, based on repetitive counts of a few foils which were recounted frequently for this purpose, it appeared that errors from this source were as large as 1%.

3. Intercalibration was necessary because several foil irradiations were made and the foils irradiated therein were counted by several different counting devices, and on different days. It was not considered feasible either to load or to count all the foils required, in a single operation. It is estimated that a standard deviation of 0.5% was encountered in intercalibration between foil runs.

4. Weighing errors of 0.3 to 0.5 mg (3 or 4%) were introduced initially into the uranium foil weight determinations because of unexpected difficulty in weighing foils within the nominal accuracy of the balance used. After this difficulty was discovered, the foils were reweighed; however, only the worst weighing errors were corrected. About 1.5% standard deviation is estimated in the weights actually incorporated into the data of this report.

5. The decay correction technique contributed a standard deviation of about 1% in the uranium fission product activities. Uranium fission product activities were decay corrected by normalization against normalizing foils which were recounted repetitively as the traverses were processed. This tended to incorporate the counting errors associated with recounting the normalizing foils into the traverse decay corrections. Part of the error was due to variable drift between the counters used, and part was attributable to counting statistics of the normalizing foils.

B. Error in Foil Placement in Core

Error in foil placement may have contributed to the relatively poor reproducibility of data. The number of measurements was increased to compensate for this. The effects of errors in vertical location were reduced by locating foils at the broad peak in the axial traverses. Lateral positioning errors as large as 0.2 cm and errors of 0.1 cm in the direction normal to the fuel plates appeared likely. The foils inside the insulating boxes could not be observed directly. No significant difference was noted between irradiations for which foils were taped to thin, loose-fitting copper strips and those for which foils were taped to or covered and inserted into thicker, snug-fitting Teflon strips. No definitive measurements

were made to determine the effect of positioning errors in the normal direction; however, the gradients were sufficiently steep to account for significant data scatter if the gradients in the normal direction extended into the voided channels between fuel plates. The lateral positioning errors could result in data errors as large as 2% in locations where flux gradients were steep (up to 10%/cm).

C. Error in Placement of Core Component

All core components were placed within 0.2 cm of their correct positions relative to the axis of the core during each run. Since the flux gradients were as large as 10%/cm about each subassembly, it would appear that 2% errors in data may have been incurred because of positioning errors of core components. This error should be more severe in regions between subassemblies, and at the interface between superheater and peripheral fuel zones, than inside the subassemblies. Also, there were visible lateral displacements of fuel plates within the insulating tubes. Insertion of snug-fitting Teflon strips and foil holders was sometimes hindered by tight coolant channels.

D. Variability of Plastic Components in Superheater

Plexiglas (Rohm & Haas unshrunk acrylic sheet) was inserted in the moderator slots of the voided superheater. This was necessary to obtain the desired location and amount of moderator. A standard variability of 4.2% was estimated from measurements of thickness of the Plexiglas near the core midplane at more or less randomly selected points. This was partly the result of local variations in thickness of individual pieces, but the piece-to-piece average thickness accounted for most of this by a standard deviation of 3.7% (weight deviation was 3.9%). The maximum or minimum thickness found in a given piece had a standard deviation from the average of that same piece of 3.4%. A number of the pieces were tapered, resulting in somewhat better than random error data at midplane among those pieces sampled.

In addition to the variability in plastic components, there were mechanical obstructions, such as seams and weld beads, in the 1.03-cm space between insulating boxes. These prevented insertion of the nominal thickness of plastic in a few locations. A good fit was indicated by a comparison of the total weight of plastic loaded with the space available.

E. Variability in Fuel Composition and Stainless Steel Content of Superheater Fuel Elements

Fuel composition variability was determined from the Special Materials Division records supplied with the superheater fuel elements. The variations in U^{235} content and stainless steel content appeared negligible in

comparison with other effects. Assembly of the fuel had been non-random. Fuel plates had been selected to obtain near-average U^{235} content in each subassembly. The actual weight of 140 fuel plates was 85.929 kg, of which 79.659 kg should have been stainless steel and 5.143 kg was U^{235}. The average U^{235} content of a 20-plate assembly (see Fig. 3) was 428.57 gm (σ = 0.046 gm or 0.01%) and the stainless steel content of the 20 fuel plates as a group was 6.638 kg (σ = 29.8 gm or 0.45%). Individual HCE fuel plates averaged 14.97 gm U^{235} (σ = 0.01 gm) and 359.43 gm stainless steel (σ = 3.7 gm) and FCE plates averaged 27.89 gm U^{235} (σ = 0.015 gm) and 356.80 gm stainless steel (σ = 3.6 gm).

VII. VOID WORTH MEASUREMENTS

Void worth measurements in the central superheater gave a reactivity loss of 2.2% ρ for the equivalent to 30% void. The actual measurements were: -0.47% ρ for one voided quadrant; -0.42% ρ for voiding the diagonally opposite quadrant; and -1.3% ρ for voiding the remaining two quadrants. The central cruciform guide sheath was worth zero to -0.01% ρ, although it introduced 3.7% void into the superheater. Measurements were by rising period increments. The excess reactivity of each core was measured (see Section IX-D) and the change from core to core was equated to the operation performed.

In Section IX-B, it may be seen that the physical void amounted to 0.277 of that of the superheater volume, including 0.037 in an ineffectual region reactivity-wise (i.e., the cruciform guide sheath). A further correction must be applied because the Plexiglas inserted in the moderator positions of the superheater had approximately 0.864 of the hydrogen density of water at room temperature. The 0.411 volume fraction of Plexiglas may be equated to 0.355 volume fraction of H_2O and 0.056 volume fraction of void, in terms of hydrogen density. Consequently, the effective void fraction of the voided core was 0.295, not including that of the cruciform sheath.

VIII. CONTROL ELEMENT CALIBRATIONS

Control blades installed initially were found to vary in worth between -0.4% and -0.7% each, depending on core conditions (see Figs. 15 and 16). When first critical with the superheater flooded (Load 145, 1228 peripheral fuel pins), all blades were equivalent at -0.053% ρ each. Voiding one quadrant of the superheater reduced the worth of the two adjacent blades to approximately -0.37% ρ each. The opposite blades appeared unaffected. The change is believed to have resulted from a flux shift away from the voided region.
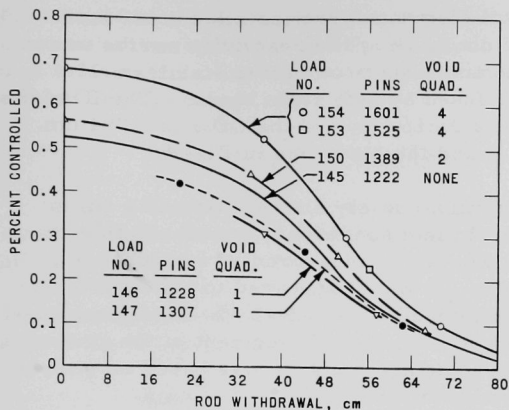
Fig. 15

Control Blade No. 5
Calibrations

Fig. 16

Control Blade No. 7
Calibrations
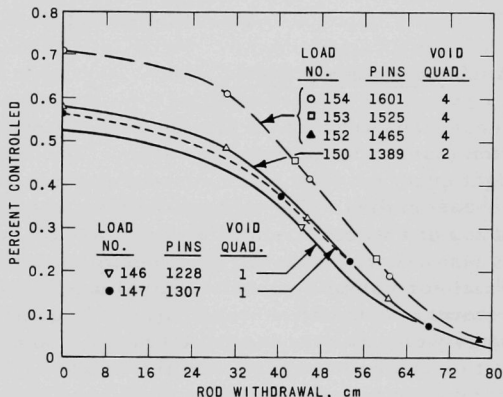
Addition of more peripheral fuel in preparation for voiding the di-
agonally opposite superheater quadrant appeared to increase the worth of
the more important blades somewhat more than the worth was increased
of the less important blades. Voiding of the second (diagonally opposite
superheater quadrant) increased all blade worths, and a further increase
was noted after the remaining two quadrants were voided. The final worths
were -0.68% ρ each for the two control blades in planes normal to the fuel
plates of the superheater, and -0.71% ρ for each of the two in parallel
planes (Load 154, 1601 peripheral fuel pins, with all superheater quadrants
voided). The control blades were 32.8 cm from the center line, or 11.5 cm
removed from the nearest edges of the quadrant cans, and this space was
filled by eight rows of peripheral fuel. Outside dimensions were 170 x
25.4 x 0.76 cm. The blades consisted of 0.635-cm-thick BORAL in an
0.06-cm-thick stainless steel sheath.

Four five-fingered control elements were installed at a 34-cm radius perpendicular to the grid diagonals. The reactivity worths were -0.21% ρ each. Each control element consisted of five stainless steel tubes filled with 90% B_4C powder fused by 10% glass binder. The ID of the Type 304 stainless steel tubes was 0.616 cm, and the OD was 0.794 cm. The locations are shown in Fig. 1 and the structure in Fig. 4.

The central cruciform cadmium safety element was 25.4 cm in span. It consisted of 0.051-cm cadmium sandwiched between 0.162-cm aluminum sheets. Its reactivity worth was measured by interchanging it with blade elements while critical. Its worth appeared to be about three times that of an individual blade element, or about -2.4%, based on measurements in the flooded core. Since only a small segment of the central safety element could be calibrated, the above figure was based on simple ratio and proportionality with the blade elements.

IX. DESCRIPTION OF CORES

A. General Description

The reactor core consisted of a central voidable superheater region (csr) and a peripheral region. The superheater included four watertight quadrant cans, each containing three BORAX-V superheater subassemblies. The subassemblies were completed except for attachment of top and bottom transition pieces, which were left off to permit ready accessibility. Since the subassemblies were to be returned to Central Shops for completion and eventual use in the BORAX-V reactor, fission product accumulation was restricted during the critical experiment. Drain plugs were situated in the bottom of each quadrant can to permit the choice of flooding and draining with the reactor vessel water level, or remaining dry during reactor operation.

The peripheral fuel was 3 w/o enriched UO_2 (in aluminum tubing) from the Hi-C supply. This fuel zone was increased in thickness until criticality was obtained (1228 Hi-C fuel pins). More fuel was added, followed by voiding a quadrant of the reactor. This was repeated for the diagonally opposite quadrant, and again for the remaining two quadrants and for installation of the central cruciform sheath.

B. Description of Superheater Region

1. Quadrant Cans

Each quadrant can enclosed three superheater subassemblies which were shimmed into position by plastic strips. The cans were approximately 20.5 x 20.5 x 106 cm in inside dimensions. Walls were

0.317-cm-thick aluminum-type 1100H14. The aluminum of one quadrant can was estimated to be 4.23 kg (in the 61-cm high active zone). There was 0.95 cm clearance between quadrant cans, forming a guide for the cruciform central safety element.

2.   Superheater Subassemblies

The superheater subassemblies were of Type 304 stainless steel. Outside dimensions were 9.23 x 9.84 x 66.5 cm, but the attachment of top and bottom caps and a pressure plate increased the dimensions to 10.07 x 10.07 x 70.47 cm. The four central subassemblies were spaced 12.19 cm center-to-center. The subassemblies in each quadrant can were spaced 10.16 cm center-to-center.

Each subassembly consisted of five insulating boxes containing four fuel plates per box. Each insulating box was 1.02 x 9.84 x 66.5 cm nominal outside dimensions and had 0.076-cm-thick walls. They were spaced 1.03 cm apart. Fuel plate dimensions were 0.076 x 9.31 x 64.1 cm, with core dimensions of 0.035 x 8.89 x 60.96 cm. They were spaced 0.23 cm center-to-center. The inner pair of fuel plates (FCE) contained 27.9 gm U^{235} each, and the outer two (HCE) contained 15.0 gm each. Fuel was highly enriched UO_2 contained in Type 304 stainless steel cermet core with Type 304 stainless steel clad.

For the entire superheater, the following weights of stainless steel were obtained by a combination of weights (which were available for fuel plates, completed subassemblies, and loose components) and dimensions: fuel plates and cladding - 79.66 kg; insulating boxes - 51.77 kg; top and bottom weldments - 25.47 kg; top and bottom caps - 21.22 kg; strips for holddown of caps - 1.86 kg; pressure plates and bolts - 2.93 kg. Only those components located within 30.5 cm of the midplane of the core were included in the figures for active zone composition given under Section (5) below. Variability in subassemblies is discussed under Sections VI-C and VI-E.

3.   Cruciform Central Sheath

Since the central cruciform element had no follower, a dry aluminum sheath was installed to displace the water between the quadrant cans. The sheath walls were slightly bowed by the static head of the surrounding water, and it is possible that as much as 0.1 cm of H_2O was present between the sheath wall and each quadrant can. (The safety element moved freely inside the sheath; consequently at least the minimum internal clearance was maintained.) Nominal dimensions were: overall span - 42 cm; thickness of a fin - 0.95 cm (slip-fit into the 0.95 cm clearance between quadrant cans); wall thickness - 0.159 cm; and the

spacer at the extremity of a fin - 0.635 cm x 0.635 cm. Weight of aluminum in the active zone (61 cm high) was estimated at 4.561 kg, of which 4.295 kg were in the walls and 0.266 kg in the spacers.

4. Plastic Moderator

Plastic pieces were packed into the moderator space inside voided quadrant cans. The minimum thickness of Plexiglas, as Rohm and Haas acrylic unshrunk sheets, between two insulating boxes was 0.873 cm nominal ($\frac{1}{4}$-, $\frac{1}{16}$-, and $\frac{1}{32}$-in. pieces, one each) or 0.827 cm average. Average weight was estimated at 616.2 gm. This accounted for ~37 kg of the total of 41.3-kg plastic in the active zone. The remainder was placed between subassemblies to shim them into position.

The weighed amount of plastic in the superheater was 41.3 kg, not including the approximate 3.5 kg in 2.54-cm-thick plastic blocks resting on top of the capped subassemblies.

Variability of plastic components is discussed under Section VI, D.

5. Superheater Composition

The composition given in Table III was calculated for the active zone of the superheater. This included all components within 30.8 cm above and below the midplane, except for the leak detector leads.

Table III

SUPERHEATER COMPOSITION

Material	Volume Fraction	Volume (liters)	Weight (kg)
U^{235}	-	-	5.143
UO_2	0.007	0.615	6.27
Aluminum (1100H14)	0.097	8.0	21.48
Stainless Steel (304)	0.206	17.0	133.3
Plastic (Plexiglas)	0.413	34.0	41.3
Void*	0.277*	22.8	-
Total	1.000	82.4	207.49

*Note that 3.01 liters (0.037 volume fraction) of void volume was in the central sheath and 19.70 liters (0.239 volume fraction) was in the quadrant cans. In terms of hydrogen content, the Plexiglas was equivalent to 0.355 volume fraction H_2O and 0.056 volume fraction of void. The effective equivalent figure is therefore 0.295 volume fraction of void in the quadrant cans, neglecting the ineffective void in the central sheath, or 0.332 including all voids.

C. 3 w/o Enrichment UO_2 Fueled Peripheral Zone

The peripheral fuel zone was 3 w/o enrichment UO_2 in Al tubing in a 1.27 cm square lattice. This fuel was from the Hi-C supply. Pellet diameter was 0.935 cm and density was 10.17 gm/cm^3. U^{235} content was 22.89 gm/fuel element or 0.188 gm/cm length in 121.9 ± 0.6 cm lengths. The UO_2 content was 853.33 gm/element (σ = 7.7 gm) or 7.0 gm/cm (σ = 0.09 gm/cm). Fuel pellets were stacked in Type 6061T-6 Al tubing of uniform OD (1.058 cm) and wall thickness (0.048 cm). Aluminum tube weights were 49.3 gm, or 0.370 gm/cm.

Table IV

COMPOSITION OF PERIPHERAL FUEL CELL

Material	Volume Fraction	Area (cm^2)	Wt/Length (av. gm/cm)	Density in Cell (av. gm/cm^3)
U^{235}	-	-	0.188	0.11656
UO_2	0.4255	0.6863	7.0	4.34
H_2O	0.4552	0.7342	0.734	0.455
Al	0.0944	0.1522	0.370	0.229
Air	0.0249	0.0402	-	-
Total	1.0000	1.6129	8.292	5.1406

D. Location of Components

1. Vertical Positioning

With the bottom of the fuel region of the superheater as a reference, the peripheral fuel extended from a point 4.4 cm below the reference point to a point 117.5 cm above the reference point. The nominal level of water moderator in the peripheral fuel was 81.0 cm above the reference point, giving 20-cm H_2O top reflector over the flooded superheater fuel region. When the superheater was voided, only 2.54 cm of Plexiglas rested above the top caps and pressure plates on the adjusting bolts.

2. Lateral Positioning

The lateral positions of the superheater components are given in part B, Description of Superheater Region. The outermost surfaces of the quadrant cans were 21.61 cm (8.51 in.) from the centerlines. The peripheral fuel was located in a 1.27-cm square lattice by insertion through grid plates. The central region was removed to permit insertion of the superheater (see Fig. 14). The nearest row of fuel pins in the peripheral

zone was at 22.86 cm (9 in.) from the centerlines, except at the indented (reentrant) quadrant corners. There they were at 12.7 cm (5 in.), and the quadrant can outer surface was at 11.45 cm (4.51 in.) from the centerline. A Plexiglas grid plate was added at the midplane to assure accurate positioning of peripheral fuel pins in the reentrant region.

E. Critical Loadings with BORAX-V Superheater

Loadings were as follows:

Load No.	Number of Hi-C Fuel Plates	Condition of Superheater	Excess Reactivity, %
145	1228	Flooded	0.77
146	1228	$\frac{1}{4}$ Voided	0.30
147	1307	$\frac{1}{4}$ Voided	0.83
148	1307	$\frac{1}{2}$ Voided	0.41
150	1389	$\frac{1}{2}$ Voided	1.30
151	1389	Voided	0.00*
152	1465	Voided	~0.73
153	1525	Voided	~1.1
156**	1465	Voided	~0.73

X. DISCUSSION OF SAFETY FEATURES
PROVIDED FOR EXPERIMENT

A. Hazards Anticipated because of Installation of Superheater

Measurements of the rate of flooding into a dummy subassembly indicated that it could be flooded completely in $\frac{1}{3}$ to $\frac{1}{2}$ sec if opened to free influx of water while submerged in an upright position. Equipment used for this measurement is shown in Fig. 17. The (dummy) superheater subassembly was mounted upright over a butterfly valve which was driven by a fast-acting rotary air cylinder. Water was drained manually from the subassembly after each test, to a level between two electrical probe locations. Water was added to the open U tube, and starting conditions

---

*It was necessary to raise the moderator above its normal depth to reach the operating flux level for Run 151-1.

**Indicated in Fig. 1. All activation measurements in the voided superheater were with this core.

corresponded with levels in the critical experiment during voided opera-
tion. An Offner recorder marked 60-cps ac-power-line phase for time
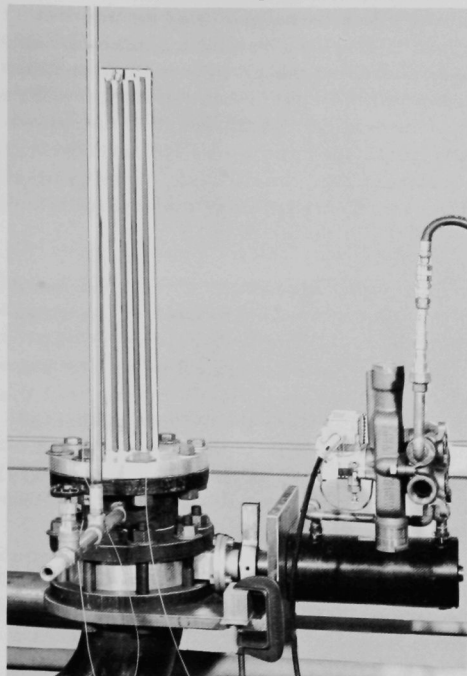base, and dry or wet potentials of the electrical probes. The times elapsed

between rise of water from the
starting level and overflow were
reproducibly recorded on the
Offner chart. It was clear that
the voided region of the super-
heater should not be installed in
a fashion which under any con-
ceivable circumstances might
permit a large portion to be
flooded so abruptly, as this would
add reactivity at a very high rate.

In addition to the flooding
mechanism, it appeared that the
voided superheater presented a
meltdown hazard because the fuel
plates were to be inside dry in-
sulating boxes rather than in con-
tact with coolant or moderator.
Consequently, only slow heat
transfer from these fuel plates
could be expected during and fol-
lowing an excursion.

It also appeared that the
prompt temperature coefficient
of the voided superheater fuel
elements would be small. The
elements contained highly en-

Fig. 17. Equipment for Measurement
of Flooding Time

riched fuel and stainless steel. Heating during an accident would result in
rapid warming of the insulated fuel, but with relatively little loss in reac-
tivity. Because of the insulated structure, relatively slow heat transfer to
the moderator would be anticipated in the superheater. Consequently,
there might be little or no boiling during an excursion.

In summary, it appeared that the introduction of the voided super-
heater region into the critical facility should be carefully planned to pre-
clude a flooding mechanism for rapid accidental insertion of reactivity.
Voiding of insulating boxes would tend to reduce the negative prompt power
coefficient. This made the choice of the peripheral fuel region relatively
restricted, as it should compensate, if possible, for the small contribution
from the superheater fuel region. Finally, the insulated superheater fuel
might melt down because of relatively slow heat transfer to other compo-
nents of the core during and following an accident.

B. Safety Features Provided for the Superheater Critical Experiment

In consideration of the flooding hazard, the superheater was divided into compartments and double water barriers were provided to prevent flooding. This included capping each of the twelve voided subassemblies individually. Quadrant cans were also installed which provided four independent primary water barriers during voided runs. Leak-detector probes were installed to scram the reactor if inleakage should occur into a quadrant can. Plastic was packed into the quadrant cans so as to limit the rate and volume of water inleakage if a quadrant can should leak. The quadrant cans were leak-tested when received from Central Shops and again before installation for voided runs.

Since access was necessary into the quadrant cans, the tops were left open and they were extended 15 cm above the water level of the reactor to insure against an accidental overflow spilling water over the top. An open pipe of 15-cm ID was installed as a positive overflow to prevent raising the water beyond the normal operating level. Rather than seal the cans at the top, close-fitting plastic plates, 2.54 cm thick, were inserted on top of the capped superheater subassemblies. It was believed that any spilled water would not seep by these plates and caps at a dangerous rate.

Safety margins adequate to shut down the reactor in its most reactive (flooded) condition were maintained at all times. The reactor would have shut down on scramming even if the most effective safety element failed to insert and the superheater flooded completely. Nevertheless, the safety system might not have acted fast enough to avert an excursion if a large part of the superheater void region could have been filled in the measured time ($\frac{1}{3}$ to $\frac{1}{2}$ sec). Consequently, it is reiterated that division into independent compartments appeared to be a fundamental safety requirement for this experiment.

The peripheral fuel zone was selected to provide a reasonably large negative prompt temperature coefficient. This tended to compensate for the small prompt coefficient of the voided superheater.

The precautions normally observed during critical experimentation were also applied. Rates of addition of reactivity were limited by control and safety rod drive speed limits and by moderator-pumping capacity. A minimum of two flux-level and one period monitors were required to be operable during all reactor operation. All scram devices were checked out for proper operation daily before operation of the reactor. Excess reactivity was built in only after it was clear that adequate shutdown margins had been installed.

C. Quadrant Can Inleakage on Run 148-3

Slow inleakage occurred in a voided quadrant during approach to critical for Run 148-3. Moisture activated a leak-detector probe in this quadrant about 3 min after moderator had been pumped into its normal operating level in the reactor vessel. The reactor was about 1% subcritical at the time of the leak-detector scram, with safety elements ready, moderator up, and one control element almost entirely withdrawn during the approach to critical. The withdrawn control and safety elements were dropped and the moderator was drained automatically on scram, bringing the reactor far subcritical without incident.

There was no observable increase in reactivity resulting from the leak. Although a control rod was being withdrawn up to the instant of the scram, it had almost reached its out-limit switch and was not increasing reactivity at a detectible rate. No increase of reactivity was detectible by examination of the flux-monitor charts.

The leaking quadrant can was removed and leak tested. Only two or three drops of water per second were leaking. This was consistent with the observed events. The bottom of the quadrant can contained visible water, but it was not thought to have reached the fuel level.

The incidence of leaks was quite unexpected inasmuch as no loading change had been made following the preceding run. Run 148-3 was to have been a continuation of control rod calibrations and intercomparisons commenced during Run 148-2, late the preceding day.

Leakage was found in two heliarc welds joining drain-plug fittings to the bottom of the leaky quadrant can. Three fittings were present in each can bottom to position the cans accurately in the base plate on which the cans rested, and to permit unrestricted inflow and outflow of moderator as the reactor vessel filled or scrammed during flooded runs. For voided runs, the drain plugs were installed, which excluded water in all cases except Run 148-3.

Investigation indicated that three (of twelve) such fittings had leaked when fabricated. Repairs had been made and satisfactory leak tests had been performed before the quadrant cans were delivered. The cans were retested on receipt at the critical experiment. Leak tests were also made by the operating crew before loading the quadrant can in voided condition for Run 148-1. Nevertheless, two of the three "repaired" welds leaked during Run 148-3. None had occurred on the preceding day.

Efforts to again repair the two leaking welds proved fruitless. The leaks recurred within a few hours, in each case. Consequently, the leaking welds were cut out and the fittings were replaced by blanks, or bosses, without drain plugs. No further leakage occurred.

ACKNOWLEDGMENTS

Although the experimental program was relatively short, many degrees of participation were necessary in planning and carrying out the BORAX-V Superheater Critical Experiment.[1] The experiment was initiated on the request of F. W. Thalgott and R. A. Rice. B. I. Spinrad and W. C. Redman provided guidance and counsel throughout the planning, hazards study, and execution of the experiment. C. N. Kelber and J. O. Juliano analyzed core characteristics and hazards of various proposals. C. E. Cohn and E. F. Groh measured the flooding rate of a dummy subassembly. L. R. Dates, R. J. Compratt, and T. W. Pienias designed modifications of the ZPR-VII (Hi-C) facility required to accommodate the superheater. E. F. Groh, J. P. Rowley, and F. F. Kodrick installed the mechanical components. R. A. Schultz designed and installed the leak-detector apparatus.

The operating personnel and their primary assignments during the experiment were: Reactor Supervisor, K. E. Plumlee,[2] with relief during vacation by Q. L. Baird[2] and W. C. Redman;[2,3] Physicists, P. I. Amundson,[10] Q. L. Baird,[2] and G. S. Stanford;[4] Technical Assistant, J. W. Armstrong;[2] Senior Technician, W. R. Robinson;[5,6] Research Technicians, F. F. Kodrick,[5,7] R. A. Schultz,[5,8] and T. A. Jensen.[9]

REFERENCES

1. K. E. Plumlee, "Critical Experiment with BORAX-V Internal Superheater," COO-267, Proceedings of the Nuclear Superheat Meeting, No. 2, 8 (April 16, 1963), p. 58.

2. K. E. Plumlee and M. T. Wiggins, Automatic Foil Activity Counting Facility and Data-reduction Program, ANL-6628 (1962).

3. D. H. Martin, Correction Factors for Cd-covered Foil Measurements, Nucleonics 13 (3), 52-53 (1955). Also NAA-SR-1076 (1954).

4. J. A. DeJuren and R. K. Paschall, Thermal Neutron Transmission through Cadmium-covered Foils, NAA-SR-7770 (1963).

5. N. P. Baumann, Resonance Integrals and Self-shielding Factors for Detector Foils, DP-817 (1963).

6. G. S. Stanford, Foil Data Thickness Corrections as Affected by Self-shielding and Flux Depression, TID-16733 (1962).

7. G. M. Jacks, A Study of Thermal and Resonance Neutron Flux Detectors, DP-608 (1961).

8. L. C. Schmid and W. P. Stinson, Lutecium as a Spectral Index Indicator, HW-66319 (1960); HW-69475, pp. 8-19 (1961); HW-74190, pp. 12-16 (1962). Also, L. C. Schmid and W. P. Stinson, Calibration of Lutecium for Measurements of Effective Neutron Temperatures, Nuclear Sci. & Eng. 7, 477-478 (1960).